Computational Mechanics 16 (1995) 297–306 © Springer-Verlag 1995

Parameter sensitivity analysis in frictional contact problems of sheet metal forming

M. Kleiber, W. Sosnowski

Abstract Influence of frictional contact effects on parameter variations of some nonlinear behaviour is studied. The flow approach to deep drawing simulation is taken as the underlying nonlinear mechanics problem. Theoretical considerations are followed by the discussion of computational aspects. In particular, difficulties resulting from parameter nondifferentiability of the response at some points along the deformation path are indicated and discussed in the computational context. An advanced numerical illustration is given.

1
Introduction

Development of formulations and numerical algorithms for the analysis of nonlinear solid and structural mechanics problems has been the subject of research activity for many decades. By now, the treatment of even those problems which are considered the most challenging, like large inelastic deformations under contact constraints, has reached a level of maturity which makes it possible to effectively address almost every complex problem of engineering analysis in this area. The natural next step on which researchers have focussed attention in the last few years is the sensitivity analysis of the nonlinear response with respect to system parameters, Tsay, Arora (1990); Vidal and Haber (1990); Chen, Hisada, Kleiber, Noguchi (1993); Kleiber (1990). The possible gains here can be phrased as follows:

(a) Gradients of functions describing system behavior with respect of parameters entering any specific theory employed are indispensable in majority of algorithms used for system optimisation, reliability and identification,

(b) It is now broadly accepted that any realistic large-scale engineering simulation has to be complemented with an extensive study on response sensitivity to system parameters just to deepen our understanding of the system behavior.

Noteworthy problems of nonlinear mechanics for which satisfactory sensitivity techniques have not yet been developed are those with unilateral constraints such as theories of plasticity with elastic range and contact/friction formulations. Particularly challenging are the latter problems – among very scare attempts to deal with them are the theoretical discussion given in Bendsoe et al. (1985) and the presentation of some algorithmic issues in Baniotopoulos and Abdalla (1995); the work of Xian Chen (1994) should also be mentioned. This paper is a next attempt to address this class of problems with emphasis on including an up-to-date contact/friction and plasticity formulation as well as on effective solving of a complex metal forming problem of engineering significance.

In Sect. 2 we briefly present equations describing the problem of deep drawing of metal sheet in the framework of the flow approach. Contact and friction effects are included. Basic concepts of the sensitivity analysis for such a formulation are discussed in Sect. 3, while Sect. 4 contains exemplary numerical studies followed by conclusions in Sect. 5.

2
Flow approach to deep drawing simulation with contact and friction effects

The flow approach to metal forming problems based on rigid-plastic and rigid-viscoplastic material model has been successfully used in practical computations for many years, Zienkiewicz, Godbole (1979); Oñate, Zienkiewicz (1983); Oñate, Kleiber, Agelet (1988); Oñate, Agelet (1992), for instance. In it, a crucial factor in accurate modelling of realistic technological problems is the way of dealing with frictional contact effects. Following Zienkiewicz, Godbole (1979); Oñate, Zienkiewicz (1983); Oñate, Agelet (1992); Wriggers, Simo, Taylor (1985); Wriggers, Van, Stein (1990) we shall briefly review below the equations describing one of the possible formulations for the sheet metal forming problem with the contact and Coulomb friction effects included in the model.

The equations describing the rigid-viscoplastic (or, as a special case, rigid-plastic) material behavior are identical to those of a non-Newtonian fluid. This justifies the use of the flow approach in which the main variables are the velocities of the deforming body defined in an Eulerian frame typical of fluid flow problems. Also, the strain rates are linearly dependent

Communicated by S. N. Atluri, 11 April 1995

M. Kleiber, W. Sosnowski
Institute of Fundamental Technological Research, Polish Academy of Science, ul. Swietokrzyska 21, 00-021 Warszawa, Poland

Correspondence to: M. Kleiber

The research on which this paper is based was partly supported by the Polish Committee for Scientific Research (KBN) under grants No 3P40401804 and 7 T08B 007 08 to the Institute of Fundamental Technologial Research, Polish Academy of Sciences, and by the International Center for Numerical Methods in Engineering (CIMNE), University Polytechnics of Catalunya, Barcelona, Spain. The support is gratefully acknowledged.

The authors appreciate the work of Professor C. Agelet de Saracibar of CIMNE who developed the program MFP2D used after some extensions in this paper.

on the velocities in a standard manner while the constitutive equation relates stress and strain rates. The problem of visco-plastic flow can be presented as follows:

equilibrium:

$$\sigma_{ij,j} = 0 \tag{1}$$

constitutive law:

$$d_{ij} = \frac{1}{2\mu^*}(\sigma_{ij} - p\delta_{ij}) = \frac{1}{2\mu^*} s_{ij} \tag{2}$$

geometric relation:

$$d_{ij} = \tfrac{1}{2}(v_{i,j} + v_{j,i}) \tag{3}$$

where σ_{ij} and s_{ij} are the Cauchy stress tensor and its deviator, respectively, p is the mean normal stress, v_i is the spatial velocity vector, d_{ij} is the rate of deformation tensor and the constitutive function (viscosity) μ^* is defined as

$$\mu^* = \frac{\bar{\sigma}}{3\dot{\bar{\varepsilon}}} = \frac{\sigma_y + \left(\frac{\dot{\bar{\varepsilon}}}{\gamma}\right)^{1/n}}{3\dot{\bar{\varepsilon}}} \tag{4}$$

Here, σ_y is the current static tensile yield limit, $\bar{\sigma}$ is the equivalent stress $\bar{\sigma} = (3/2 s_{ij}s_{ij})^{1/2}$, $\dot{\bar{\varepsilon}}$ is the effective inelastic strain rate, $\dot{\bar{\varepsilon}} = (2/3 d_{ij}d_{ij})^{1/2}$ and γ, n are parameters of the model. For strain hardening materials the yield limit σ_y is a function of the effective inelastic strain $\bar{\varepsilon}$, $\sigma_y = \sigma_y(\bar{\varepsilon})$; $\bar{\varepsilon}$ has to be computed as the time integral $\dot{\bar{\varepsilon}}$.

It is interesting and extremely useful computationally to observe that the structure of the above equations is anologous to that of standard incompressible infinitesimal elasticity, the differences being (a) displacements and strain velocities replacing displacements and strains themselves and (b) the constitutive function μ^* replacing the elastic shear modulus μ. The analogy has a great computational potential since it allows to treat advanced plastic flow using computer software developed for linear elasticity. To do so one has simply to allow the elastic shear modulus μ to be a given function of the current yield stress σ_y and the current effective strain rate $\dot{\bar{\varepsilon}}$, and to interpret the displacements u_i as the instantenous velocities v_i. The fact that the underlying material is incompressible may cause some difficulties in dealing with bulk forming processes in 3D or plane strain, Antunez, Idelson (1990) – it is of no concern in solving sheet forming problems such as those discussed in this paper.

For the virtual velocity field v satisfying appropriate kinematic boundary conditions the 3D virtual work equation reads

$$\int_{\Omega} \boldsymbol{\sigma}^T_{1\times 6}\mathbf{d}_{6\times 1}d\Omega = \int_{\Omega} \hat{\mathbf{f}}^T_{1\times 3}\mathbf{v}_{6\times 3}d\Omega + \int_{d\Omega_\sigma} \hat{\mathbf{t}}^T_{1\times 3}\mathbf{v}_{3\times 1}d(d\Omega) \tag{5}$$

which upon introducing the finite element expansion

$$\mathbf{v}_{3\times 1} = \boldsymbol{\varphi}_{3\times N}\dot{\mathbf{q}}_{N\times 1} \tag{6}$$

$$\mathbf{d}_{6\times 1} = \mathbf{B}_{6\times N}\dot{\mathbf{q}}_{N\times 1} \tag{7}$$

with $\dot{\mathbf{q}}_{N\times 1}$ as nodal velocities, yields

$$\int_{\Omega} \mathbf{B}^T_{N\times 6}\boldsymbol{\sigma}_{6\times 1}d\Omega = \mathbf{Q}_{N\times 1} \tag{8}$$

with

$$\mathbf{Q}_{N\times 1} = \int_{\Omega} \boldsymbol{\varphi}^T_{N\times 3}\hat{\mathbf{f}}_{3\times 1}d\Omega + \int_{d\Omega_\sigma} \boldsymbol{\varphi}^T_{N\times 3}\hat{\mathbf{t}}_{3\times 1}d(d\Omega) \tag{9}$$

Using Eqs. (2), (6) and (8) becomes

$$\left(\int_{\Omega} 2\mu^*\mathbf{B}^T_{N\times 6}\mathbf{B}_{6\times N}d\Omega\right)\dot{\mathbf{q}}_{N\times 1} + \int_{d\Omega_\sigma} p\mathbf{B}^T_{N\times 6}\mathbf{1}_{6\times 1}d\Omega = \mathbf{Q}_{N\times 1} \tag{10}$$

in which

$$\mathbf{1}_{6\times 1} = \{1\ \ 1\ \ 1\ \ 0\ \ 0\ \ 0\} \tag{11}$$

On account of the incompressibility constraint

$$tr\,\mathbf{d} = \mathbf{1}^T_{1\times 6}\mathbf{B}_{6\times N}\dot{\mathbf{q}}_{N\times 1} = 0 \quad \text{for any} \quad \dot{\mathbf{q}}_{N\times 1} \tag{12}$$

Eq. (10) becomes

$$\left(\int_{\Omega} 2\mu^*\mathbf{B}^T_{N\times 6}\mathbf{B}_{6\times N}d\Omega\right)\dot{\mathbf{q}}_{N\times 1} = \mathbf{Q}_{N\times 1} \tag{13}$$

or shorter

$$\mathbf{K}_{N\times N}(\mu^*)\dot{\mathbf{q}}_{N\times 1} = \mathbf{Q}_{N\times 1} \tag{14}$$

where

$$\mu^* = \mu^*(\dot{\bar{\varepsilon}}, \sigma_y, \gamma, n)$$

$$\dot{\bar{\varepsilon}} = \dot{\bar{\varepsilon}}(\dot{\mathbf{q}})$$

$$\sigma_y = \sigma_y(\bar{\varepsilon}) \tag{15}$$

are known functions of the respective arguments. The stiffness matrix K depends on the solution $\dot{\mathbf{q}}$ through the viscosity parameter μ^* so that an iterative process is generally needed to find the solution vector $\dot{\mathbf{q}}$. Experiences with solving forming problems described by Eq. (14) show, Antunez, Idelsohn (1990), that the Newton-Raphson iteration scheme is applicable (i.e. it converges) only for markedly rate-dependent materials (steel in hot working conditions) for which $n < 2$ in Eq. (4). Otherwise the direct iteration based on

$$\mathbf{K}^{(i)}\dot{\mathbf{q}}^{(i+1)} = \mathbf{Q} \quad i = 0, 1, 2, \ldots \tag{16}$$

in which

$$\mathbf{K}^{(i)} = \mathbf{K}(\mu^*(\dot{\mathbf{q}}^{(i)})) \tag{17}$$

is preferred even if is only linearly convergent. (Procedures for accelerating convergence have been proposed by Antunez, Idelsohn (1990)).

Using the Newton-Raphson scheme we have the i-th residual

$$\mathbf{R}^{(i)} = \mathbf{Q} - \mathbf{K}^{(i)}\dot{\mathbf{q}}^{(i)} \tag{18}$$

while the correction $\delta\dot{\mathbf{q}}^{(i)}$ such that

$$\dot{\mathbf{q}}^{(i+1)} = \dot{\mathbf{q}}^{(i)} + \delta\dot{\mathbf{q}}^{(i)} \tag{19}$$

is computed from

$$\mathbf{R}^{(i+1)} \cong \mathbf{R}^{(i)} + \frac{\partial \mathbf{R}^{(i)}}{\partial \dot{\mathbf{q}}^{(i)}}\delta\dot{\mathbf{q}}^{(i)} = \mathbf{0} \tag{20}$$

i.e. as

$$\delta\dot{\mathbf{q}}^{(i)} = -\left(\frac{\partial \mathbf{R}^{(i)}}{\partial \dot{\mathbf{q}}^{(i)}}\right)^{-1}\mathbf{R}^{(i)} = \mathbf{K}_T^{(i)-1}\mathbf{R}^{(i)} \tag{21}$$

where

$$\frac{\partial \mathbf{R}^{(i)}}{\partial \dot{\mathbf{q}}^{(i)}} = \frac{\partial \mathbf{Q}}{\partial \dot{\mathbf{q}}} - \left(\mathbf{K}^{(i)} + \int_\Omega 2(\mathbf{B}^T\mathbf{B}\dot{\mathbf{q}}^{(i)})\frac{\partial \mu^*}{\partial \dot{\mathbf{q}}^{(i)}}\,d\Omega\right) = -\mathbf{K}_T^{(i)} \tag{22}$$

is the (non-symmetric) tangent stiffness matrix while

$$\frac{\partial \mu^*}{\partial \dot{\mathbf{q}}^{(i)}} = \frac{\partial \mu^*}{\partial \dot{\bar{\varepsilon}}}\frac{\partial \dot{\bar{\varepsilon}}}{\partial \mathbf{d}}\frac{\partial \mathbf{d}}{\partial \dot{\mathbf{q}}} = \frac{\left[-\sigma_y + \left(\frac{1}{n} - 1\right)\left(\frac{\dot{\bar{\varepsilon}}}{\gamma}\right)^{1/n}\right]}{3\dot{\bar{\varepsilon}}^3}2\mathbf{B}^T\mathbf{B}\dot{\mathbf{q}} \tag{23}$$

If quasi-stationary problems are considered no time integration enters; otherwise, for an implicit scheme the computation of the load term $\partial\mathbf{Q}/\partial\dot{\mathbf{q}}$ contribution to the tangent stiffness matrix may be required. To better see that difference between the Newton-Raphson and direct iteration we rewrite Eq. (16) as

$$\mathbf{K}^{(i)}\delta\dot{\mathbf{q}}^{(i)} = \mathbf{R}^{(i)} \tag{24}$$

where $\delta\dot{\mathbf{q}}^{(i)}$ and $\mathbf{R}^{(i)}$ are given by Eqs. (19) and (18) respectively.

The class of sheet forming sensitivity problems we aim at solving allows to employ the axisymmetric shell theory as developed in metal forming context by Oñate and Zienkiewicz (1983). In fact, the analogy of the flow equations to those of infinitesimal elasticity makes it possible to replace any standard elastic formulation by the one describing rigid-viscoplastic forming problem. An approach of this kind was successfully employed by Oñate and Zienkiewicz (1983); details of it are not repeated here for brevity.

It should be also emphasized that the deep drawing problems are inherently transient and application of the flow approach methodology, best suited for steady-state situations requires appropriate re-interpretation and numerical treatment. The reader is referred to Oñate and Zienkiewicz (1983) for detailed description of the algorithm used to this purpose.

Description of contact effects is essential for realistic modeling of many technological problems related to sheet metal forming. A brief description of a formulation discussed by Wriggers, Simo, Taylor (1985), Wriggers, Van, Stein (1990) which is broadly considered most accurate and effective is given below under a number of simplifying assumptions relevant to the problem on hand. The assumptions are as follows:

- 2D problems are considered only,
- one of the contacting bodies is rigid resulting in the unilateral constraints imposed on the motion of the metal sheet considered,
- the boundary of the rigid body is approximated by a collection of straight linear segments,
- the linear Coulomb friction law is assumed.

Let us consider a slave node 's' of the deforming body that is likely to penetrate a master segment of the rigid body defined by the nodes 'm1', 'm2', Fig. 1. The so-called gap function is defined at the point 's' as

$$g_s = (\mathbf{x}_s - \mathbf{x}_{m1})\mathbf{n} \tag{25}$$

where $\mathbf{n}$ denotes the unit normal to the master segment, $\mathbf{x}_s$ is the current position of the slave node 's' and $\mathbf{x}_{m1}$ is the (constant) position of the master node 'm1'.

The inequality

$$g_s \geqq 0 \tag{26}$$

has to be checked for all candidate contact nodes 's' from the finite set S, $s \in S$. In general, S will contain all the boundary nodes of the deforming body. For $g_s \leqq 0$ the constraint equation for the node 's' becomes active ($s \in S_A$); otherwise, the constraint is inactive ($s \in S_I$). The length of the master segment is defined as

$$l = \|\mathbf{x}_{m2} - \mathbf{x}_{m1}\| \tag{27}$$

while the unit vector tangent to the segment as

$$\mathbf{t} = \frac{1}{l}(\mathbf{x}_{m2} - \mathbf{x}_{m1}) \tag{28}$$

We are looking for a solution to the problem at a fixed time instant $t + \Delta t$ assuming that the solution up to the preceding time instant t inclusive has already been obtained. The iteration number at the time step considered is denoted by 'i', as before.

The contact constraint condition (26) at time $t + \Delta t$ and iteration 'i' reads

$${}^{t+\Delta t}g_s^{(i)} = ({}^{t+\Delta t}\mathbf{x}_s^{(i)} - \mathbf{x}_{m1})^T\mathbf{n} \geqq 0 \tag{29}$$

which at the $(i+1)$-th iteration becomes

$$\begin{aligned} {}^{t+\Delta t}g_s^{(i+1)} &= ({}^{t+\Delta t}\mathbf{x}_s^{(i)} + \delta\mathbf{u}_s^{(i)} - \mathbf{x}_{m1})^T\mathbf{n} \\ &= {}^{t+\Delta t}g_s^{(i)} + \delta\mathbf{u}_s^{(i)T}\mathbf{n} = {}^{t+\Delta t}g_s^{(i)} + \delta g_s^{(i)} \end{aligned} \tag{30}$$

where to simplify notation the index '$t + \Delta t$' is dropped in all symbols denoting variations.

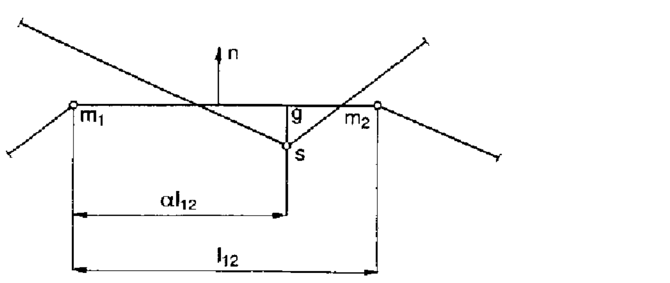

Fig. 1. Geometry of the slave nodes with a master segment m1–m2

To effectively use (30) in the framework of the flow approach the change in the gap function has to be expressed in terms of the nodal velocities by using a time integration scheme of the form, for instance

$$ {}^{t+\Delta t}\mathbf{x}_s^{(i+1)} = {}^{t+\Delta t}\mathbf{x}_s^{(i)} + \theta \Delta t \delta \dot{\mathbf{q}}_s^{(i)} \quad 0 \leqq \theta \leqq 1 \tag{31} $$

or

$$ \delta \mathbf{u}_s^{(i)} = \theta \Delta t \delta \dot{\mathbf{q}}_s^{(i)} \tag{32} $$

where θ is a parameter of the integration scheme while

$$ \delta \dot{\mathbf{q}}_s^{(i)} = {}^{t+\Delta t}\dot{\mathbf{q}}_s^{(i+1)} - {}^{t+\Delta t}\dot{\mathbf{q}}_s^{(i)} \tag{33} $$

The expression (33) is a straightforward consequence of the relationship

$$ \begin{aligned} {}^{t+\Delta t}\mathbf{x}_s^{(i+1)} &= {}^{t}\mathbf{x}_s + \Delta t\, {}^{t}\dot{\mathbf{q}}_s + \theta \Delta t ({}^{t+\Delta t}\dot{\mathbf{q}}_s^{(i+1)} - {}^{t}\dot{\mathbf{q}}_s) \\ &= {}^{t}\mathbf{x}_s + (1-\theta)\Delta t\, {}^{t}\dot{\mathbf{q}}_s + \theta \Delta t\, {}^{t+\Delta t}\dot{\mathbf{q}}_s^{(i+1)} \end{aligned} \tag{34} $$

The so-called perturbed Lagrangian function is adopted in the discretized form for one 'e'-th finite element with N_e degrees of freedom and with just one node 's' in contact as

$$ \Pi_\varepsilon({}^{t+\Delta t}\dot{\mathbf{q}}^{(i+1)}, {}^{t+\Delta t}\lambda^{(i+1)}) = \tilde{\Pi}({}^{t+\Delta t}\dot{\mathbf{q}}^{(i+1)}) + {}^{t+\Delta t}\lambda_s^{(i+1)}\, {}^{t+\Delta t}g_s^{(i+1)} - \frac{1}{2\varepsilon}\lambda_s^{(i+1)}\lambda_s^{(i+1)} \tag{35} $$

in which ε is a parameter, $\tilde{\Pi}$ can be given an interpretation in terms of the element potential energy associated with the incremental deformation with the velocity ${}^{t-\Delta t}\dot{\mathbf{q}}^{(i+1)}$

$$ \tilde{\Pi}({}^{t+\Delta t}\dot{\mathbf{q}}^{(i+1)}) = \tfrac{1}{2}\, {}^{t+\Delta t}\dot{\mathbf{q}}^{(i+1)T}\, {}^{t+\Delta t}\mathbf{K}_{(e)}^{(i)}\, {}^{t+\Delta t}\dot{\mathbf{q}}^{(i+1)} - {}^{t+\Delta t}\mathbf{Q}_{(e)}^{T^{(i)}}\, {}^{t+\Delta t}\dot{\mathbf{q}}^{(i+1)} \tag{36} $$

and λ_s is the contact force normal component at node 's' (due to the assumption of frictionless contact only the normal component of the force appears in the formulation). The velocity vector $\dot{\mathbf{q}}_s$ is assumed to be related to the vector of the element nodal velocities by means of the transformation

$$ \dot{\mathbf{q}}_{s2\times 1} = \mathbf{A}^{(e)}_{2\times N_e}\dot{\mathbf{q}}_{N_e\times 1} \tag{37} $$

The velocity at the node 's' has to satisfy the constraint

$$ {}^{t+\Delta t}g_s^{(i+1)} = g_s^{(i)} + \mathbf{n}^T \theta \Delta t \delta \dot{\mathbf{q}}_s^{(i)} \geqq 0 \tag{38} $$

Stationary conditions for the functional Π_ε

$$ \delta_q \Pi_\varepsilon = \frac{\partial \Pi_\varepsilon}{\partial \dot{\mathbf{q}}^{(i+1)}}\hat{\delta}\dot{\mathbf{q}} = 0 \tag{39} $$

$$ \delta_\lambda \Pi_\varepsilon = \frac{\partial \Pi_\varepsilon}{\partial \lambda^{(i+1)}}\hat{\delta}\lambda = 0 \tag{40} $$

for any admissible $\hat{\delta}\dot{\mathbf{q}}$, $\hat{\delta}\lambda$, yields the equations

$$ \left(\frac{\partial \tilde{\Pi}}{\partial^{t+\Delta t}\dot{\mathbf{q}}_s^{(i+1)}} + {}^{t+\Delta t}\lambda^{(i+1)} \frac{\partial^{t+\Delta t} g_s^{(i+1)}}{\partial^{t+\Delta t}\dot{\mathbf{q}}^{(i+1)}} \right) \hat{\delta}\dot{\mathbf{q}} = 0 \tag{41} $$

$$ \left({}^{t+\Delta t}g_s^{(i+1)} - \frac{1}{\varepsilon}\, {}^{t-\Delta t}\lambda_s \right) \hat{\delta}\lambda = 0 \tag{42} $$

which read more explicitely

$$ {}^{t+\Delta t}_{(e)}\mathbf{K}_T^{(i+1)}\, {}^{t-\Delta t}\dot{\mathbf{q}}^{(i+1)} - {}^{t+\Delta t}\mathbf{Q}_{(e)}^{T^{(i)}} + ({}^{t+\Delta t}\lambda_s^i + \hat{\delta}\lambda_s^i)\, \mathbf{A}^{(e)T}_{sN_e\times 2}\mathbf{n}_{2\times 1}\theta \Delta t = 0 \tag{43} $$

$$ {}^{t+\Delta t}g_s^{(i+1)} - \frac{1}{\varepsilon}({}^{t+\Delta t}\lambda_s^{(i)} + \hat{\delta}\lambda_s^{(i)}) = 0 \tag{44} $$

By linearising the equations at $({}^{t+\Delta t}\dot{\mathbf{q}}^{(i+1)}, {}^{t+\Delta t}\lambda^i)$ and noting that, cf. Eqs. (18), (33)

$$ \begin{aligned} {}^{t+\Delta t}_{(e)}\mathbf{K}_T^{(i)}\, {}^{t+\Delta t}\dot{\mathbf{q}}^{(i+1)} - {}^{t+\Delta t}_{(e)}\mathbf{Q}^{T^{(i)}} &= {}^{t+\Delta t}_{(e)}\mathbf{K}_T^{(i+1)}\hat{\delta}\dot{\mathbf{q}}^{(i)} - {}^{t+\Delta t}_{(e)}\mathbf{Q}^{T^{(i)}} + {}^{t+\Delta t}_{(e)}\mathbf{K}_T^{(i+1)}\, {}^{t+\Delta t}\dot{\mathbf{q}}^{(i+1)} \\ &= {}^{t+\Delta t}_{(e)}\mathbf{K}_T^{(i+1)}\hat{\delta}\dot{\mathbf{q}}^{(i)} - {}^{t-\Delta t}_{(e)}\mathbf{R}^{(i)} \end{aligned} \tag{45} $$

we obtain

$$ \begin{bmatrix} {}^{t+\Delta t}_{(e)}\mathbf{K}_T^{(i)} & \mathbf{A}_s^{(e)^T}\mathbf{n}\theta\Delta t \\ \mathbf{n}^T\mathbf{A}_s^{(e)^T}\theta\Delta t & -\frac{1}{\varepsilon} \end{bmatrix} \begin{bmatrix} \hat{\delta}\dot{\mathbf{q}}^{(i)} \\ \hat{\delta}\lambda_s^{(i)} \end{bmatrix} = \begin{bmatrix} {}_{(e)}\mathbf{R}^{(i)} - \lambda_s^{(i)}\mathbf{A}_s^{(e)^T}\mathbf{n}\theta\Delta t \\ \frac{1}{\varepsilon}\lambda_s^{(i)} - g_s^{(i)} \end{bmatrix} \tag{46} $$

By solving the second equation for $\hat{\delta}\lambda_s^{(i)}$

$$ \hat{\delta}\lambda_s^{(i)} = \varepsilon(g_s^{(i)} + \mathbf{n}^T\mathbf{A}_s^{(e)}\hat{\delta}\dot{\mathbf{q}}^{(i)}\mathbf{n}\theta\Delta t) - \lambda_s^{(i)} \tag{47} $$

and substituting it in the first equation, we obtain

$$ [{}^{t+\Delta t}_{(e)}\mathbf{K}_T^{(i)} + \varepsilon\mathbf{A}_s^{(e)^T}\mathbf{n}\mathbf{n}^T\mathbf{A}_s^{(e)}(\theta\Delta t)^2]\hat{\delta}\dot{\mathbf{q}}^{(i)} = {}_{(e)}\mathbf{R}^{(i)} - \varepsilon\mathbf{A}_s^{(e)^T}\mathbf{n}g_s^{(i)}\theta\Delta t \tag{48} $$

or

$$ [{}^{t+\Delta t}_{(e)}\mathbf{K}_T^{(i)} + {}_{(e)}\mathbf{K}_{c_s}]\hat{\delta}\dot{\mathbf{q}}^{(i)} = {}_{(e)}\mathbf{R}^{(i)} + {}_{(e)}\mathbf{R}_{c_s}^{(i)} \tag{49} $$

The quantities

$$ {}_{(e)}\mathbf{K}_{c_sN_e\times N_e} = \varepsilon\mathbf{A}_s^{(e)^T}{}_{N_e\times 2}\mathbf{n}_{2\times 1}\mathbf{n}^T_{1\times 2}\mathbf{A}_s^{(e)}(\theta\Delta t)^2 \tag{50} $$

$$ {}_{(e)}\mathbf{R}^{(i)}_{c_sN_e\times 1} = \varepsilon\mathbf{A}_s^{(e)^T}{}_{N_e\times 2}\mathbf{n}_{2\times 1}g_s^{(i)}\theta\Delta t \tag{51} $$

are the contributions to the element tangent stiffness matrix and tangent residual force vector due to contact. The expressions (50), (51) have been derived relative to a single slave node 's' coming into contact with a master segment. The matrix $\mathbf{K}_{c_s}$ is symmetric. In forming the global stiffness matrix and the global residual force vector all the contributions due to contact have to be accounted for in the course of the usual assembly process. Observing the global ordering of nodes and interelement connection we may symbolically write

$$\mathbf{R}_c = \sum_{s \in S_A} \mathbf{R}_{c_s} \tag{52}$$

$$\mathbf{K}_c = \sum_{s \in S_A} \mathbf{K}_{c_s} \tag{53}$$

The global system of FEM equations becomes

$$[\mathbf{K}_T^{(i)} + \mathbf{K}_c^{(i)}]\,\hat{\delta}\dot{\mathbf{q}}^{(i)} = \mathbf{R}^{(i)} + \mathbf{R}_c^{(i)} \tag{54}$$

If in the iteration scheme the secant $\mathbf{K}^{(i)}$ rather than tangent stiffness matrix $\mathbf{K}_T^{(i)}$ is employed in Eq. (54), only the linear convergence can be expected. On the other hand, the consistent way in which $\mathbf{K}_c$ and $\mathbf{R}_c$ have been obtained assures quadratic convergence provided the iteration is based on Eq. (54).

So far, frictionless contact effects have been discussed. Limiting ourselves to the linear Coulomb friction law we postulate the tangent force residual in the form, cf Eq. (51)

$$_{(e)}\mathbf{R}_{f_s} = -\mu\varepsilon \mathbf{A}_s^{(e)^T}{}_{N_e \times 2}\mathbf{t}'_{2\times 1} g_s \theta \Delta t \tag{55}$$

in which

$$\mathbf{t}' = \mathbf{t}\,sgn(\dot{\mathbf{q}}_s) = \frac{\dot{\mathbf{q}}^{slip}}{\|\dot{\mathbf{q}}^{slip}\|} \tag{56}$$

Variation of the expression $\hat{\delta}\dot{\mathbf{q}}^T\mathbf{R}_{f_s}$ with respect to ${}^{t+\Delta t}\dot{\mathbf{q}}^{(i+1)}$ gives

$$\frac{\partial(\hat{\delta}\dot{\mathbf{q}}^T\mathbf{R}_{f_s})}{\partial\dot{\mathbf{q}}}\delta\dot{\mathbf{q}} = -\mu\varepsilon\theta\Delta t\hat{\delta}\dot{\mathbf{q}}^T\mathbf{A}_s^{(e)^T}\left(\frac{\partial\mathbf{t}'}{\partial\dot{\mathbf{q}}}g_s + \mathbf{t}'\frac{\partial g_s}{\partial\dot{\mathbf{q}}}\right)\delta\dot{\mathbf{q}} \tag{57}$$

By observing the relation, cf. Wriggers, Simo, Taylor (1985),

$$\frac{\partial\mathbf{t}'}{\partial\dot{\mathbf{q}}}\hat{\delta}\dot{\mathbf{q}} = \frac{1}{\|\dot{\mathbf{q}}_s^{slip}\|}\left[\frac{\partial\dot{\mathbf{q}}_s^{slip}}{\partial\dot{\mathbf{q}}}\hat{\delta}\dot{\mathbf{q}} - \mathbf{t}'\frac{\partial\|\dot{\mathbf{q}}^{slip}\|}{\partial\dot{\mathbf{q}}}\hat{\delta}\dot{\mathbf{q}}\right]$$

$$= \frac{1}{\|\dot{\mathbf{q}}_s^{slip}\|}(1 - \mathbf{n}\mathbf{n}^T - \mathbf{t}\mathbf{t}^T)\mathbf{A}_s^{(e)}\hat{\delta}\dot{\mathbf{q}} \tag{58}$$

which vanishes for 2D problems, and the relation

$$\frac{\partial g_s}{\partial\dot{\mathbf{q}}}\hat{\delta}\dot{\mathbf{q}} = \theta\Delta t\mathbf{n}^T\hat{\delta}\dot{\mathbf{q}}_s = \theta\Delta t\mathbf{n}^T\mathbf{A}_s^{(e)}\hat{\delta}\dot{\mathbf{q}} \tag{59}$$

we obtain from Eq. (57)

$$\frac{\partial(\hat{\delta}\dot{\mathbf{q}}^T\mathbf{R}_{f_s})}{\partial\dot{\mathbf{q}}}\hat{\delta}\dot{\mathbf{q}} = \hat{\delta}\dot{\mathbf{q}}^T\mathbf{K}_{f_s}\hat{\delta}\dot{\mathbf{q}} \tag{60}$$

where

$$\mathbf{K}_{f_s} = -\mu\varepsilon(\theta\Delta t)^2\mathbf{A}_s^{(e)^T}\mathbf{t}'\mathbf{n}^T\mathbf{A}_s^{(e)^T} \tag{61}$$

is the non-symmetric contribution to the element stiffness matrix due to friction at the node 's'.

Similarly as before in Eq. (52), the global quantities due to friction result as

$$\mathbf{R}_f = \sum_{s \in S_A} \mathbf{R}_{f_s} \tag{62}$$

$$\mathbf{K}_f = \sum_{s \in S_A} \mathbf{K}_{f_s} \tag{63}$$

while the final system of the FEM equations becomes

$$(\mathbf{K}_T^{(i)} + \mathbf{K}_c^{(i)} + \mathbf{K}_f^{(i)})\,\delta\dot{\mathbf{q}}^{(i+1)} = \mathbf{R}^{(i)} + \mathbf{R}_c^{(i)} + \mathbf{R}_f^{(i)} \tag{64}$$

This system of equations, after appropriate specification to the shell problem on hand, allows to iteratively determine the unknown velocity field ${}^{t+\Delta t}\dot{\mathbf{q}}^{(i-1)}$. If, as observed before, secant stiffness matrix $\mathbf{K}^{(i)}$ rather than $\mathbf{K}_T^{(i)}$ is to be employed, then Eq. (64) is used in the form

$$(\mathbf{K}^{(i)} + \mathbf{K}_c^{(i)} + \mathbf{K}_f^{(i)})\,\delta\dot{\mathbf{q}}^{(i+1)} = \mathbf{R}^{(i)} + \mathbf{R}_c^{(i)} + \mathbf{R}_f^{(i)} \tag{65}$$

in which the non-symmetric contribution to the tangent stiffness matrix, cf. Eq. (22)

$$\tilde{\mathbf{K}} = \int_\Omega 2\mathbf{B}^T\mathbf{B}\dot{\mathbf{q}}^{(i)}\frac{\partial\mu^*}{\partial\dot{\mathbf{q}}^{(i)}}\mathrm{d}\Omega \tag{66}$$

has been neglected in the iteration matrix.

A simple procedure to deal with friction can be based on the iterative adjustment of nodal reactions in contact nodes at the blank-tool interfaces until they satisfy a Coulomb type of friction law, Michalowski, Mroz (1978), for instance.

Convergence and others problems appear when relatively small strain velocity increments with different signs for neighboring nodal points are observed. As can be seen from Fig. 2, in which the classical and a regularized Coulomb rule is presented, the Coulomb law may give very different friction forces for nodes sliding over rigid surfaces with almost the same velocity. Even for nodes with "proper" sliding direction

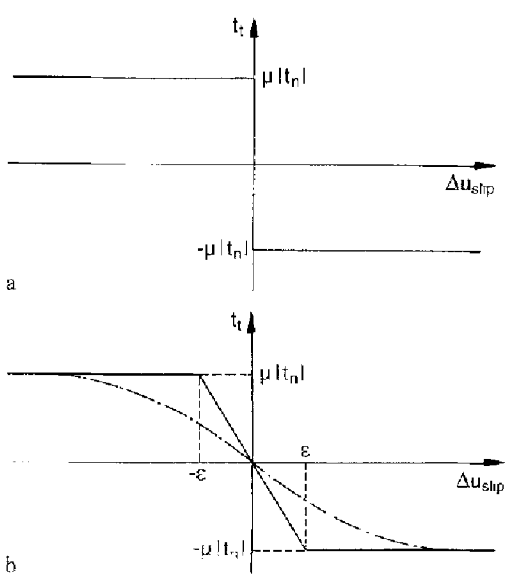

Fig. 2a, b. Coulomb friction layes **a** classical, **b** regularized different friction tractions result from different slip values and "artificial wrinkling" is produced.

Coulomb friction law is usually expressed as

$$\Delta \mathbf{u}^{slip} = \mathbf{0} \quad \text{if} \quad |\mathbf{f}_t| < \mu |\mathbf{f}_n| \tag{67}$$

$$\Delta \mathbf{u}^{slip} = -\lambda |\mathbf{f}_t| \quad \text{if} \quad |\mathbf{f}_t| = \mu |\mathbf{f}_n| \tag{68}$$

where $\Delta \mathbf{u}^{slip}$ denotes relative sliding between two contact points, λ is a positive scalar, $\mathbf{f}_n$ is the normal contact force and $\mathbf{f}_t$ is the tangent contact force which may be treated as reaction to sliding. Condition (67) corresponds to stick (sliding impossible) while condition (68) to a possible sliding.

Additional regularization of the Coulomb law is necesary to avoid "artificial wrinkling".

Algorithmic issues relevant to the computer code used in this study were thoroughly explained by Sosnowski (1993 and 1994). In particular, the slip condition for those neighboring nodal points at which small strain velocities increments with different signs are observed is replaced by the stick condition.

3
Parameter sensitivity analysis

For linear (and some nonlinear) problems assessment of the response 1-st order sensitivity to parameter variation means finding the response gradient with respect to the parameter. However, for complex problems involving inequality constraints (such as those due to contact and friction) the sensitivity information carried by the gradient is limited. In fact, this class of problems is inherently nonlinear and nondifferentiable, and a more sophisticated mathematics leading to Gateaux differentials (directional derivatives) is needed to properly address the sensitivity problem. In this paper just one parameter (the coefficient of friction) is considered so that the sensitivity results based on the gradient information are believed to be useful provided they are interpreted with sufficient care as explained later in this section.

With h as any parameter entering the theory we consider a functional whose sensitivity with respect to the parameter is to be assessed, in the form

$$\Phi = \Phi[\mathbf{s}(h), \dot{\mathbf{q}}(h); h] \tag{69}$$

the dependence of Φ on its argument (but not of the stress deviator $\mathbf{s}$ and $\dot{\mathbf{q}}$ on h) assumed known. In the present 'non-shape' sensitivity considerations h may be taken as one of the following parameters: n, γ, σ_o, μ, ε in all or some integration points in the region analysed. For brevity, we confine ourselves to deriving sensitivity equations for just one parameter h – a more general case of sensitivity defined as the directional derivative with respect to a vector of the parameters directly follows the pattern set by the simple discussion.

Employing the so-called direct differentiation method we differentiate Eq. (69) with respect to h to get the functional sensitivity as

$$\frac{d\Phi}{dh} = \frac{\partial \Phi}{\partial h} + \frac{\partial \Phi}{\partial \mathbf{s}}\frac{d\mathbf{s}}{dh} + \frac{\partial \Phi}{\partial \dot{\mathbf{q}}}\frac{d\dot{\mathbf{q}}}{dh} \tag{70}$$

in which $\partial\Phi/\partial h$, $\partial\Phi/\partial \mathbf{s}$ and $\partial\Phi/\partial\dot{\mathbf{q}}$ can be routinely (i.e. by a simple function evaluation) obtained for the given solution $(\dot{\mathbf{q}}, \mathbf{s})$ while $d\mathbf{s}/dh$ can be expressed as, cf. Eq. (2)

$$\frac{d\mathbf{s}}{dh} = \frac{d\mathbf{s}}{d\dot{\mathbf{q}}}\frac{d\dot{\mathbf{q}}}{dh} = 2\mu^* \bar{\mathbf{B}}\frac{d\dot{\mathbf{q}}}{dh} + 2\frac{\partial \mu^*}{\partial \dot{\mathbf{q}}}\frac{d\dot{\mathbf{q}}}{dh} + \bar{\mathbf{B}}\dot{\mathbf{q}} \tag{71}$$

Therefore, for the known solution $(\dot{\mathbf{q}}, \mathbf{s})$, only $d\dot{\mathbf{q}}/dh$ needs to be obtained from additional considerations in order to determine $d\Phi/dh$. To this aim we consider first the non-contact problem, i.e.

$$\mathbf{K}[\mu^*(\dot{\mathbf{q}}, h)]\,\dot{\mathbf{q}}(h) = \mathbf{Q}(h) \tag{72}$$

The formulation can be extended by allowing the right-hand side vectors depend additionally on $\dot{\mathbf{q}}(h)$ – it has not been done here in the interest of brevity only.

Differentiating Eq. (72) with respect to h gives

$$\frac{d\mathbf{K}}{dh}\dot{\mathbf{q}} + \mathbf{K}\frac{d\dot{\mathbf{q}}}{dh} = \frac{d\mathbf{Q}}{dh} \tag{73}$$

$$\frac{d\mathbf{K}}{dh} = \frac{d\mathbf{K}}{d\mu^*}\frac{d\mu^*}{dh} = \frac{d\mathbf{K}}{d\mu^*}\left(\frac{d\mu^*}{dh} + \frac{d\mu^*}{d\dot{\mathbf{q}}}\frac{d\dot{\mathbf{q}}}{dh}\right) \tag{74}$$

$$\left(\mathbf{K} + \frac{d\mathbf{K}}{d\mu^*}\dot{\mathbf{q}}\right)\frac{d\mu^*}{d\dot{\mathbf{q}}}\frac{d\dot{\mathbf{q}}}{dh} = \frac{d\mathbf{Q}}{dh} - \frac{d\mathbf{K}}{d\mu^*}\frac{d\mu^*}{dh}\dot{\mathbf{q}} \tag{75}$$

$$\mathbf{K}_T\frac{d\dot{\mathbf{q}}}{dh} = \frac{d\mathbf{Q}}{dh} - \frac{d\mathbf{K}}{d\mu^*}\frac{d\mu^*}{dh}\dot{\mathbf{q}} \tag{76}$$

By using the definition of the residual given in Eq. (18) we obtain

$$\mathbf{K}_T\frac{d\dot{\mathbf{q}}}{dh} = \left.\frac{d\mathbf{R}}{dh}\right|_{\dot{\mathbf{q}} \neq \dot{\mathbf{q}}(h)} \tag{77}$$

in which the notation on the right-hand side is meant to indicate that the derivative should be computed under the assumption of the velocities $\dot{\mathbf{q}}$ independent of the parameter h. As a consequence, the right-hand side vector can be computed provided the primary (equilibrium) problem has been solved; the velocity sensitivity vector $d\dot{\mathbf{q}}/dh$ then follows by solving Eq. (77) which is linear and does not require iteration. Clearly, the latter property has fundamental significance in terms of computational efficiency.

The right-hand side vector in Eq. (77) can be presented more explicitely by noting that

$$\frac{d\mathbf{K}}{d\mu^*} = \int_\Omega 2\mathbf{B}^T\mathbf{B}\,d\Omega \tag{78}$$

$$\frac{d\mu^*}{dh} = \frac{\partial \mu^*}{\partial \dot{\mathbf{q}}}\frac{d\dot{\mathbf{q}}}{dh} + \frac{\partial \mu^*}{\partial h} \tag{79}$$

The DDM based sensitivity Eq. (77) can be extended to account for contact and friction effects by observing Eq. (64). Before doing this we have to point out again that an obvious difficulty in effective computation of the sensitivity gradient in such a case is that problems with unilateral constraints are generally non-differentiable and only directional derivatives exist. This is definitely a complication which apparently invalidates the standard sensitivity technique based upon the straightforward differentiation of the problem equations with respect to the parameter on hand. However, as results from the theoretical discussion of Bendsoe et al. (1985) the kinematic variables are not differentiable with respect to the parameter only if some active constraints are associated with zero reactions forces – a situation which can hardly be expected in finite element analysis of large-scale problems. Thus, we effectively assume differentiability of the response – even if it is theoretically unsatisfactory the results are believed to be correct within the general finite element accuracy.

By analogy to Eq. (77) the sensitivity equation reads now

$$(\mathbf{K}_T + \mathbf{K}_c + \mathbf{K}_f)\frac{d\dot{\mathbf{q}}}{dh} = \frac{d}{dh}[\mathbf{R} + \mathbf{R}_c + \mathbf{R}_f]|_{\dot{\mathbf{q}} \neq \mathbf{q}(h)} \tag{80}$$

which can be effectively used to compute sensitivity of any functinal via Eq. (70). In the above equation the following notation was used

$$\mathbf{R}_c = \sum_{s \in S_A} -\varepsilon \mathbf{A}_s^{(e)^T} \mathbf{n} g_s \theta \Delta t \tag{81}$$

$$\mathbf{R}_f = \sum_{s \in S_A} -\mu\varepsilon \mathbf{A}_s^{(e)^T} \mathbf{t}' g_s \theta \Delta t \tag{82}$$

In the context of the sensitivity analysis the question arises whether the actual tangent matrix $\mathbf{K}_T$ or the stiffness matrix $\mathbf{K}$, Eq. (17) should be used for finding $d\dot{\mathbf{q}}/dh$ by Eq. (77). Using Eq. (80) as it is written above has the great advantage of resulting in the non-iterative solution for $d\dot{\mathbf{q}}/dh$. However, as indicated in Sect. 2 the tangent matrix $\mathbf{K}_T$ may quite often be unavailable because of the equilibrium iteration algorithm based on $\mathbf{K}$; Eq. (80) should then be rewritten as

$$(\mathbf{K} + \mathbf{K}_c + \mathbf{K}_f)\frac{d\dot{\mathbf{q}}}{dh} = \frac{d}{dh}[\mathbf{R} + \mathbf{R}_c + \mathbf{R}_f]|_{\dot{\mathbf{q}} \neq \mathbf{q}(h)} - \tilde{\mathbf{K}}\frac{d\dot{\mathbf{q}}}{dh} \tag{83}$$

for which the direct iteration scheme reads

$$(\mathbf{K} + \mathbf{K}_c + \mathbf{K}_f)\frac{d\dot{\mathbf{q}}^{(j+1)}}{dh} = \frac{d}{dh}[\mathbf{R} + \mathbf{R}_c + \mathbf{R}_f]|_{\mathbf{q} \neq \mathbf{q}(h)} - \tilde{\mathbf{K}}\frac{d\dot{\mathbf{q}}^{(j)}}{dh} \tag{84}$$

We thus obtain the sensitivity equation which is an alternative to Eq. (80). It removes some drawbacks of Eq. (80) ($\mathbf{K}_T$ in practical applications is frequently nearly singular) at the cost of having to iterate to find $d\dot{\mathbf{q}}/dh$.

By specifying the parameter h we can readily derive explicit expressions for the right-hand side vector in Eq. (80) or Eq. (81). Observing that

$$\left.\frac{d^{t+\Delta t}g_s}{dh}\right|_{^{t+\Delta t}\mathbf{q} \neq \dot{\mathbf{q}}(h)} = \frac{\partial g_s}{\partial \mathbf{x}_s}\frac{d\mathbf{x}_s}{dh} = \mathbf{n}\left[\frac{d^t\mathbf{x}_s}{dh} + (1-\theta)\Delta t\frac{d^t\dot{\mathbf{q}}_s}{dh}\right]$$

$$= \mathbf{n}\left[\frac{d^t\mathbf{x}_s}{dh} + (1-\theta)\Delta t \mathbf{A}^e \frac{d^t\dot{\mathbf{q}}}{dh}\right] \tag{85}$$

we obtain the respective non-zero terms as follows:

for $h = \mu$

$$\left.\frac{d\mathbf{R}_c}{d\mu}\right|_{^{t+\Delta t}\mathbf{q} \neq \mathbf{q}(\mu)} = \sum_{s \in S_A} -\varepsilon \mathbf{A}_s^{(e)^T}\mathbf{n}\left\{\mathbf{n}\left[\frac{d^t\mathbf{x}_s}{d\mu} + (1-\theta)\Delta t \mathbf{A}^e \frac{d^t\dot{\mathbf{q}}}{d\mu}\right]\right\}\theta\Delta t \tag{86}$$

$$\left.\frac{d\mathbf{R}_f}{d\mu}\right|_{^{t+\Delta t}\mathbf{q} \neq \mathbf{q}(\mu)} = -\sum_{s \in S_A} \varepsilon \mathbf{A}_s^{(e)^T}\mathbf{t}' g_s \theta\Delta t - \sum_{s \in S_A} \varepsilon \mathbf{A}_s^{(e)^T}\mathbf{t}' \cdot \left\{\mathbf{n}\left[\frac{d^t\mathbf{x}_s}{d\mu} + (1-\theta)\Delta t \mathbf{A}^e \frac{d^t\dot{\mathbf{q}}}{d\mu}\right]\right\}\theta\Delta t \tag{87}$$

for $h = \varepsilon$

$$\left.\frac{d\mathbf{R}_c}{d\varepsilon}\right|_{^{t+\Delta t}\dot{\mathbf{q}} \neq \dot{\mathbf{q}}(\varepsilon)} = -\sum_{s \in S_A} \mathbf{A}_s^{(e)^T}\mathbf{n} g_s \theta\Delta t - \sum_{s \in S_A} \mathbf{A}_s^{(e)^T}\mathbf{n} \cdot \left\{\mathbf{n}\left[\frac{d^t\mathbf{x}_s}{d\varepsilon} + (1-\theta)\Delta t \mathbf{A}^e \frac{d^t\dot{\mathbf{q}}}{d\varepsilon}\right]\right\}\theta\Delta t \tag{88}$$

$$\left.\frac{d\mathbf{R}_f}{d\varepsilon}\right|_{^{t+\Delta t}\mathbf{q} \neq \dot{\mathbf{q}}(\varepsilon)} = \sum_{s \in S_A} -\mu \mathbf{A}_s^{(e)^T}\mathbf{t}' g_s \theta\Delta t - \sum_{s \in S_A} \mu \mathbf{A}_s^{(e)^T}\mathbf{t}' \cdot \left\{\mathbf{n}\left[\frac{d^t\mathbf{x}_s}{d\varepsilon} + (1-\theta)\Delta t \mathbf{A}^e \frac{d^t\dot{\mathbf{q}}}{d\varepsilon}\right]\right\}\theta\Delta t \tag{89}$$

for $h = \gamma$

$$\left.\frac{d\mathbf{R}}{d\gamma}\right|_{\dot{\mathbf{q}} \neq \dot{\mathbf{q}}(\gamma)} = \left(\int_\Omega 2\mathbf{B}^T\mathbf{B}\dot{\mathbf{q}}^{(i)}\frac{1}{3n\bar{\dot{\varepsilon}}\gamma}\left(\frac{\bar{\dot{\varepsilon}}}{\gamma}\right)^{(1/n)-1} d\Omega\right)\dot{\mathbf{q}}^{(i)} \tag{90}$$

for $h = n$

$$\left.\frac{d\mathbf{R}}{dn}\right|_{\mathbf{q} \neq \dot{\mathbf{q}}(\gamma)} = -\left(\int_\Omega 2\mathbf{B}^T\mathbf{B}\frac{1}{3\bar{\dot{\varepsilon}}n^2}\left(\frac{\bar{\dot{\varepsilon}}}{\gamma}\right)^{1/n}\ln\left(\frac{\bar{\dot{\varepsilon}}}{\gamma}\right)d\Omega\right)\dot{\mathbf{q}}^{(i)} \tag{91}$$

The assumption made above that each of the parameters is the same at every integration point or node can obviously be removed so that sensitivity can easily be analysed with respect to a parameter defined at just one point in system, for instance. We also note that in accordance with the assumption of Sect. 3 the vectors $\mathbf{n}$ and $\mathbf{t}'$ are considered independent of h.

Having solved Eq. (80) or Eq. (84) for $d^{t-\Delta t}\dot{\mathbf{q}}_s/dh$ the updating of $d\mathbf{x}_s/dh$ follows according to

$$\frac{d^{t+\Delta t}\mathbf{x}_s}{dh} = \frac{d^t\mathbf{x}_s}{dh} + \Delta t\left[(1-\theta)\frac{d^t\dot{\mathbf{q}}_s}{dh} + \theta\frac{d^{t+\Delta t}\dot{\mathbf{q}}_s}{dh}\right] \tag{92}$$

Both $d^{t+\Delta t}\dot{\mathbf{q}}_s/dh$ and $d^{t+\Delta t}\mathbf{x}_s/dh$ have to be stored for the next step computations.

4
Example – stretching of circular blank with hemispherical punch

The stretching of a thin circular, isotropic sheet with a hemispherical punch is considered.

The geometrical configuration of the problem, tools geometry, deformed sheet shape at the punch travel of 1.17

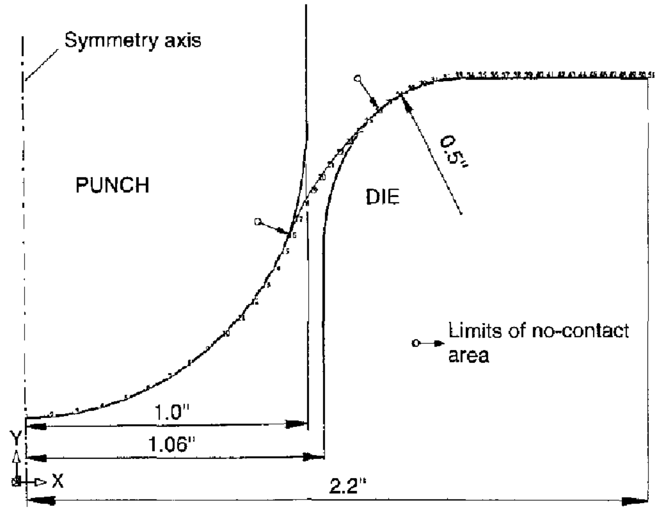

Fig. 3. Hemispherical punch stretching problem. Tools geometry. Deformed shape and nodal points numbers

inches and its node numbers are shown in Fig. 3. Limits of the no-contact area are marked in this figure as well. The blank has the initial overall radius of 2.2 inches. The coefficient of friction for the basic problem is $\mu = 0.04$.

50 uniformly distributed axisymmetric shell elements are used for the analysis, Oñate and Agelet (1992). The finite element program MFP2D described by Oñate and Agelet (1992) and extended by the second author of this paper is employed.

The uniaxial stress-strain curve for the matrix material is given by

$$\sigma = 5.4 + 27.8\varepsilon^{0.504}, \quad \frac{ton}{in^2}, \quad \text{for} \quad \varepsilon \leq 0.36 \tag{93}$$

$$\sigma = 5.4 + 24.4\varepsilon^{0.504}, \quad \frac{ton}{in^2}, \quad \text{for} \quad \varepsilon > 0.36 \tag{94}$$

In Fig. 4(c) sensitivity of the horizontal nodal velocities with respect to the friction coefficient calculated by using the direct

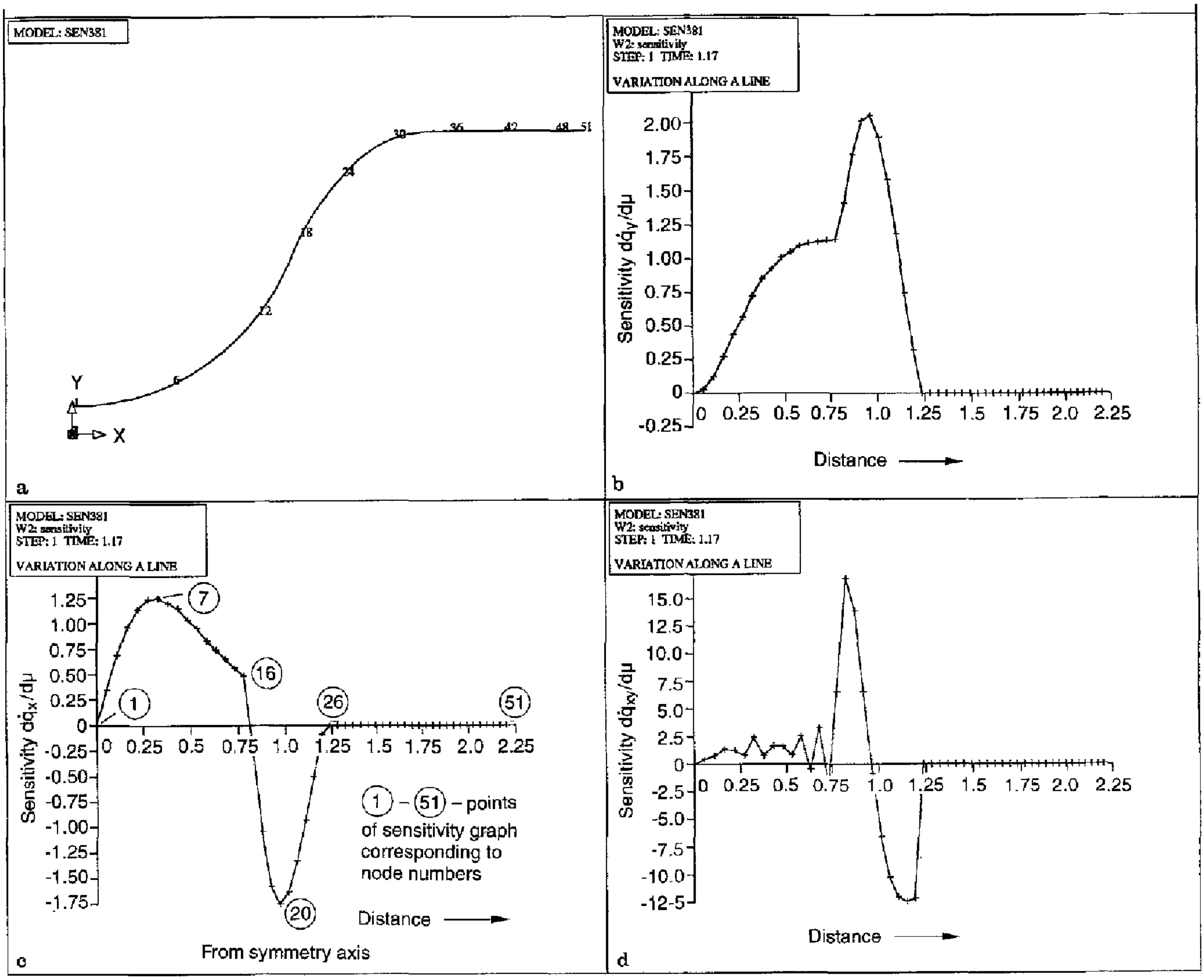

Fig. 4a–d. Hemispherical punch stretching problem. **a** deformed shape of the shell at the punch travel of 1.17 inches, **b** sensitivity of the nodal vertical velocities with respect to the friction coefficient at $q_{1y} = 1.17$", calculated by DDM, **c** sensitivity of the nodal horizontal velocities with respect to the friction coefficient at $q_{1y} = 1.17$", calculated by DDM, **d** sensitivity of the nodal rotational velocities with respect to the friction coefficient at $q_{1y} = 1.17$", calculated by DDM

differentiation method (DDM) for punch travel of $q_{1y} = 1.17$ inches is presented. Sensitivity values corresponding to the sheet node numbers given in the previous figure are shown. One can observe that the maximal sensitivity of $\dot{q}_x$ with respect to friction corresponds to the nodal point number 7 being in contact with the punch surface. Also a negative sensitivity area in the no-contact zone can be observed. Increasing the value of the friction coefficient results in decreasing horizontal velocity in this area as a compensation of the opposite effect occuring over the punch surface.

A remarkable fact is that no finite difference sensitivity solution (out of many attempted) has resulted in a reliable approximation of the sensitivity values. Small parameter perturbations have resulted in excessive round-off errors, as the velocities fields for basic and disturbed solutions, respectively differ very little, while larger perturbations have induced unacceptable truncation errors. Thus, once again, and similarly as in the sensitivity analysis of linear systems, Haftka, Gurdal (1992) the so-called analytical approach to sensitivity appears not only more cost-effective but the only reliable way of assessing sensitivity.

In Fig. 4 the following additional information is presented: (a) deformed shape of the shell at the punch travel q_{1y} of 1.17 inches, (b) sensitivity of the nodal vertical velocities with respect to the friction coefficient at $q_{1y} = 1.17$", (d) sensitivity of the nodal rotational velocities with respect to the friction coefficient at $q_{1y} = 1.17$".

Sensitivity of the horizontal nodal velocities with respect to the friction coefficient calculated by the direct differentiation method (DDM) for three increasing punch travels q_{1y} is presented in Fig. 5. As expected, the results indicate that the response sensitivity decreases with the process development. The greatest sensitivity is observed at the beginning of the process. The sensitivity solution has been obtained using the tangent rather than secant stiffness matrix as described in Sect. 3. The solution, generally less stable than that obtained with the secant stiffness matrix, has not converged at early stages of the process so that the latter had to be employed initially.

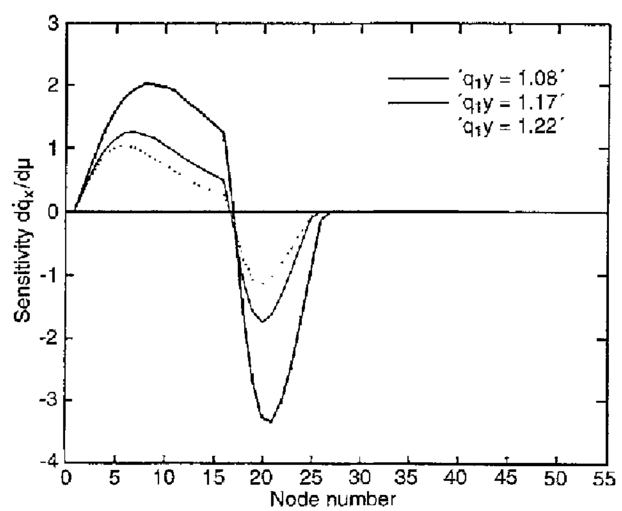

Fig. 5. Hemispherical punch stretching problem. Sensitivity of the horizontal velocity component against friction by direct differentiation method (DDM) for different punch travels

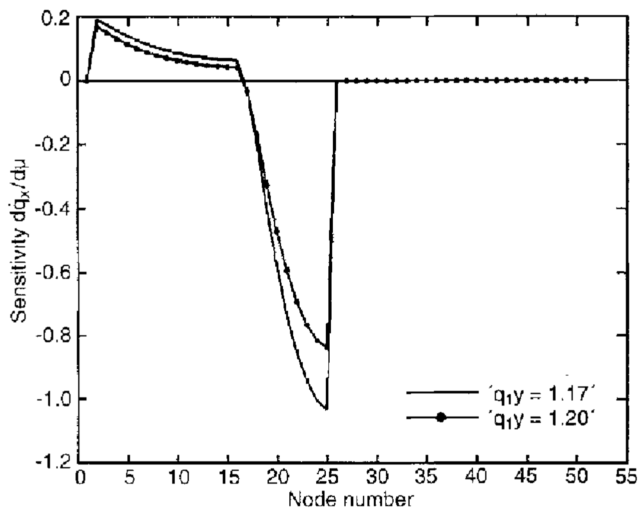

Fig. 6. Hemispherical punch stretching problem. Re-defined sensitivity of the horizontal velocity component against friction by direct differentiation method (DDM)

A useful way of presenting the results is by re-defining the sensitivity variable to a non-dimensional form as $\mu/\dot{q}_x$, $d\dot{q}_x/d\mu$, Fig. 6. Such values provide an interesting information indicating the relative functional (i.e. the appropriate velocity component) change due to the relative change of the system parameter.

5
Conclusions

1. In the paper an important, but so far very rarely treated in the computational mechanics literature, area of nonlinear parameter sensitivity studies has been identified and discussed.
2. A practical approach to the sensitivity analysis for contact/ friction problems has been developed and tested numerically.
3. The method can easily be implemented into existing finite codes provided they are available in the source form.
4. For effective optimization, reliability and identification of nonlinear systems with unilateral constraints further studies on sensitivity formulations appear urgently needed–non-differentiable problems for which only directional derivatives exist deserve special attention.

References

Antunez, H. J.; Idelsohn, S. R. 1990: Topics in numerical solution of isothermal and thermal-coupled forming processes, Latin Amer. Appl. Res. 20: 69–89

Baniotopoulos, C. C.; Abdalla, K. M. 1995: Sensitivity analysis results on the separation problem of bolted steel column-to-column connections, Int. J. Solids Structures 32(2): 251–265

Bendsoe, M. P.; Olhoff, N.; Sokolowski, J. 1985: Sensitivity analysis of problems of elasticity with unilateral constraints, J. Struct. Mech. 13(2): 201–222

Chen, X. 1994: Nonlinear finite element sensitivity analysis for large deformation elastoplastic and contact problems, Ph. D. Thesis, Univ. of Tokyo, Japan

Chen, X.; Hisada, T.; Kleiber, M.; Noguchi, H. 1992: Comparison of different sensitivity analysis algorithms for large deformation elasto-plastic problems, Design Sensitivity Analysis, in Kleiber, M.; Hisada, T. eds, Atlanta Technology Publications 52–67

Haftka, R. T.; Gurdal, Z. 1992: Elements of Structural Optimalization, Kluwer Academic Publishers

Kleiber, M. 1993: Shape and nonshape structural design sensitivity analysis for problems with any material and kinematic nonlinearity, Comp. Meth. Appl. Mech. Eng. 81: 183–208

Michalowski, R.; Mroz, Z. 1978: Associated and non-associated sliding rules in contact friction problems, Archives of Mechanics 30: 259–276

Oñate, E.; Agelet de Saracibar, C. 1992: Numerical modelling of sheet metal forming problems in P. Hartley et al. (Eds.), Numerical Modelling of Material Deformation Process, Spinger-Verlag

Oñate, E.; Kleiber, M.; Agelet de Saracibar, C. 1988: Plastic and viscoplastic flow of void containing metals: Applications to axisymmetric sheet forming problems, Int. J. Num. Meth. Engng. 25: 225–251

Oñate, E.; Zienkiewicz, O. C. 1983: A viscous shell formulation for the analysis of thin sheet metal forming, Int. J. Mech. Sci. 25: 305–335

Sosnowski, W. 1993: Approximate friction treatment in sheet metal forming simulation, Archives of Mechanics 45(5): 595–614

Sosnowski, W. 1994: Flow approach – finite element model for stamping processes versus experiment, Computer Assisted Mechanics and Engineering Sciences 1: 49–75

Tsay, J. J.; Arora, J. S. 1990: Nonlinear structural design sensitivity analysis for path dependent problems Part I General theory, Comp. Meth. Appl. Mech. Eng. 81: 183–208

Vidal, C. A.; Haber, R. B. 1990: Design sensitivity analysis for rate independent elasto-plasticity, Comp. Meth. Appl. Mech. Eng. 81: 183–208

Wriggers, P.; Simo, J. C.; Taylor, R. L. 1985: Penalty and augmented Lagrangian Formulations for contact problems, Proc. NUMETA'85 A. A. Balkena, 97–106

Wriggers, P.; Vu Van, T.; Stein, E. 1990: Finite elements formulation of large Deformation Impact-Compact problems, 37: 319–331